Interaction of 5–50 MeV/nucleon ^{3}He and ^{4}He with ^{59}Co

J. Jastrzębski
Heavy Ion Laboratory, Warsaw University, Warsaw, Poland
and Indiana University Cyclotron Facility, Bloomington, Indiana 47405

P. P. Singh, T. Mróz,* S. E. Vigdor, and M. Fatyga
Indiana University Cyclotron Facility, Bloomington, Indiana 47405

H. J. Karwowski
Indiana University Cyclotron Facility, Bloomington, Indiana 47405
and Department of Physics and Astronomy, University of North Carolina, Chapel Hill, North Carolina 27514
(Received 25 November 1985)

Excitation functions and thick target recoil ranges for radioactive nuclei produced in ^{3}He and ^{4}He bombardment of ^{59}Co over a 5–50 MeV/nucleon energy range have been measured using the activation technique. At 81 and 118 MeV ^{4}He energy, the angular distributions of the radioactive recoils were also measured. Using the in-beam gamma ray technique, production cross sections for many radioactive as well as stable residual nuclei were measured for the ^{4}He + ^{59}Co system for a ^{4}He energy range between 30 and 150 MeV. Close to 90% of the reaction cross section was observed over the entire energy range. From the experimental data, information about the energy and linear momentum deposition in the interaction of He projectiles with the Co target was gathered. Two distinct changes in the reaction mechanism are apparent at about 40 and 90 MeV bombarding energies, as manifested by observables related to the energy and momentum deposition. The change of the reaction mechanism at 40 MeV is related to the onset of preequilibrium α-particle and nucleon emission. The nature of the mechanism change which sets in at 90 MeV is less well understood.

I. INTRODUCTION

This paper continues a series of reports on gross features of the interaction of intermediate energy light projectiles with medium mass nuclei. The experiments have been performed at the Indiana University Cyclotron Facility. Gamma ray spectroscopy techniques were used to determine the cross sections of final heavy reaction residues, their recoil ranges, and in some cases their angular distributions. In previous publications we have reported and discussed the data pertaining to the interaction of 80–160 MeV protons with Ni isotopes,[1–3] and to the 10–100 MeV ^{6}Li interaction with Fe targets.[4] In the present work ^{3}He and ^{4}He induced reactions on a ^{59}Co target are presented and compared to our previous results with p and ^{6}Li projectiles. Partial results of this study were recently published.[5,6]

In the energy range relevant to the present work the ^{4}He + ^{59}Co reaction was previously investigated by Michel and Brinkmann[7] (E_α from 20 MeV up to 173 MeV) and Gadioli *et al.*[8] (E_α from 10 MeV up to 85 MeV). In these works the cross sections of radioactive products were determined using the stacked foil technique. A similar method was employed by Michel and Glas[9] to deduce the cross sections in ^{3}He induced reactions on a ^{59}Co target in the energy range 14–130 MeV.

The excitation functions of the radioactive products observed in these reactions contain some information about the mechanism of the interaction of He projectiles with Co nuclei. Indeed, in Refs. 7–9 these excitation functions were compared with preequilibrium-plus-evaporation model calculations, and various reaction mechanisms were indicated as contributing to the production of final, radioactive nuclei.

As has been shown in a number of recent papers (see, e.g., Refs. 10 and 11), one of the most important observables which describes the reaction mechanism characteristics for ions with energies above 10 MeV/nucleon is the linear momentum transfer (LMT) from projectile to the targetlike products. Different fractions of the available linear momentum are generally transferred in fusionlike, preequilibrium particle emission and direct reactions. The variation of LMT with increasing bombarding energy may give some insight into the evolution of the reaction mechanism and perhaps reveal new phenomena. Moreover, the information about the LMT puts an additional (as compared with residual nuclide excitation functions alone) constraint on reaction model calculations. The linear momentum transfer can be easily obtained from any cascade model calculation and recently was also extracted from the preequilibrium-plus-evaporation models.[12,13]

In the present work a particular emphasis is put on investigation of the linear momentum characteristics in the ^{4}He- and ^{3}He-induced reactions on ^{59}Co, employing the classical method of thick-target recoil range measurements.[14] Additionally, supplementary information was gathered about the cross sections of radioactive and stable reaction products. The latter results allow us to obtain complete mass distributions of the reaction residues and

to deduce from them the average removed mass, a quantity which is related to the energy deposition.

Three types of experiments are presented here, all based on gamma-ray counting techniques using high resolution Ge(Li) detectors. First, for six α-particle bombarding energies we have determined the cross sections of the radioactive as well as stable products by detecting in-beam gamma rays characteristic for the reaction products. The advantages and shortcomings of this method when applied to light projectiles in the mass region around $A=60$ have been discussed previously.[2,4]

In the second type of experiment the stacked-foil technique was used to determine cross sections and thick-target recoil ranges for the radioactive products in ^{3}He- and ^{4}He-induced reactions. This method was previously used in our investigation of proton (Ref. 3) and ^{6}Li (Ref. 4) induced reactions in the same mass region. Cross sections were obtained from the radioactivity measurements with much higher precision than those obtained from the in-beam data. Previously, some thick target recoil ranges were obtained using the ^{4}He beam from the Groningen cyclotron[15,16] and, in general, these data were in good agreement with the results presented here. They were, however, limited to a smaller α-particle energy range and had somewhat larger experimental uncertainties.

Finally, for two α-particle bombarding energies we have determined the angular distributions of the radioactive recoils. These measurements provided necessary verification of assumptions used in evaluating the linear momentum parallel to the beam direction which is deduced from the thick-target recoil ranges.

The ensemble of these experimental data has allowed us to gather information about the energy and linear momentum deposition in ^{3}He and ^{4}He induced reactions on a ^{59}Co target, over an energy range in which one expects[17] the projectile-nucleus interaction to evolve from one dominated by the mean field of the target nucleus toward another one in which an increasingly prominent role is played by individual nucleon-nucleon collisions.

II. EXPERIMENTAL METHODS AND RESULTS

The experimental methods used in the present work are in many respects analogous to those described in detail in our previous publications, particularly in Ref. 4. We refer the reader to this paper for further details not listed here.

A. Beams and targets

The He^{++} beams from the variable energy accelerator system at the Indiana University cyclotron were accelerated up to the maximum available energy for ^{4}He ions (200 MeV) and up to 140 MeV for ^{3}He ions. The on-line γ-ray measurements (see Sec. II B) were performed using a beam of about 1 electric nA incident upon 5 mg/cm^2 thick targets in the low intensity target station. The transmitted beam was collected in a three section Faraday cup, and its total charge was measured using a calibrated charge integrator. For one bombarding energy (149.5 MeV), after the in-beam counting, the γ-ray spectra of the irradiated target were additionally measured off-line for residual activity during a period of several weeks. In this way, after the correction for recoils, the absolute values of the cross section of radioactive reaction products were compared with those obtained in the hot-cell irradiation areas, where a different Faraday cup was used (see below).

Samples for off-line residual radioactivity measurements (see Sec. II C) were produced using 100–200 electric nA beams of the He^{++} ions in the hot cell irradiation area. The target assemblies consisted generally of a stack of Co foils (each about 5–6 mg/cm^2 thick) and Al forward and backward catchers interspersed with Al beam energy degraders. Up to seven target-catcher combinations were used for a given bombardment. In a few cases a single target-catcher sample was irradiated. The beam current measurements were performed by collecting the charge from the thick Al beam stopper, placed close to the target area. In the case of the ^{4}He beam the Al catchers as well as the beam degraders were also used as beam monitors through the production of ^{22}Na (see Sec. II C). The beam energy along the stack was calculated using formulae from Ref. 18. In addition, this energy was checked at the end of the stack by comparing the ratios of the cross sections for different radioactive products from the stack segment (after a substantial beam energy degradation) with those obtained in a single target bombardment, where the beam energy value was read from the cyclotron setting. Stopping power coefficients used to calculate the degraded energy were adjusted by a few percent to make these ratios agree.

B. In-beam cross section determinations

The cross sections of the radioactive and stable products for the ^{4}He+^{59}Co reaction are listed in Table I. The indicated errors originate mainly from ambiguities in as-

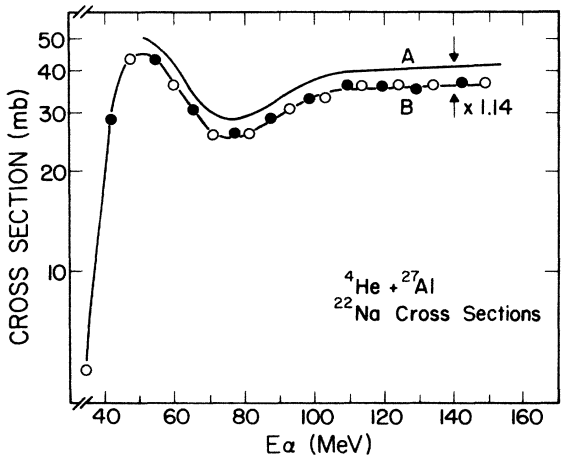

FIG. 1. The cross section for the production of ^{22}Na from Al targets by ^{4}He ions. Curve A: data from Ref. 19. Curve B: present work; closed circles are from thick beam degraders, open circles from thin Al catchers. The lines are drawn to guide the eye. Curves A and B coincide in the high energy region if the ordinate of curve B is multiplied by a factor of 1.14.

TABLE I. Cross sections (in mb) for $^{4}He+^{59}Co$ reaction products determined from the in-beam γ-ray measurements.

Product	E_{lab} (MeV) 30.3	39.9	49.0	65.7	127.3	149.5
^{62}Cu	48 (7)	21 (5)	8 (3)	3 (3)		
^{61}Cu	418 (30)	70 (10)	30 (5)	23 (10)		
^{60}Cu	56 (15)	32 (8)	23 (4)	6 (2)		
^{59}Cu		6 (6)	10 (10)	8 (4)		
^{62}Ni	45 (20)	30 (30)	6 (6)			
^{61}Ni	344 (60)	197 (15)	64 (15)	21 (5)		
^{60}Ni	122 (10)	549 (30)	480 (25)	169 (15)	22 (4)	25 (5)
^{59}Ni	69 (25)	68 (25)	165 (20)	224 (20)	87 (8)	54 (12)
^{58}Ni	17 (17)	15 (15)	20 (20)	35 (10)	20 (4)	16 (3)
^{61}Co	20 (5)	14 (5)				
^{60}Co	5 (5)	26 (6)	38 (13)	18 (8)		
^{59}Co	43 (10)	129 (12)	182 (40)	169 (15)	58 (8)	91 (18)
^{58}Co	151 (15)	113 (9)	87 (10)	125 (10)	121 (8)	138 (15)
^{57}Co	7 (3)	69 (5)	110 (15)	50 (10)	26 (7)	56 (16)
^{56}Co	2 (2)	4 (2)	8 (4)	41 (4)	23 (5)	31 (5)
^{59}Fe						8 (8)
^{58}Fe	1 (1)	13 (3)	6 (3)	7 (4)	18 (6)	26 (4)
^{57}Fe		53 (15)	100 (20)	67 (15)	76 (16)	175 (30)
^{56}Fe		5 (2)	58 (10)	191 (8)	160 (10)	270 (20)
^{55}Fe			5 (5)	26 (10)	47 (6)	95 (15)
^{54}Fe					18 (4)	43 (5)
^{53}Fe					2 (1)	4 (2)
^{55}Mn	2 (1)	4 (2)	2 (2)	6 (2)	37 (5)	40 (20)
^{54}Mn		5 (2)	25 (5)	16 (5)	93 (6)	92 (10)
^{53}Mn			3 (3)	23 (4)	24 (4)	62 (5)
^{52}Mn					10 (5)	10 (5)
^{51}Mn					12 (3)	13 (3)
^{54}Cr					5 (2)	10 (10)
^{53}Cr					6 (3)	13 (11)
^{52}Cr					23 (3)	48 (6)
^{51}Cr					17 (4)	32 (6)
^{50}Cr					7 (2)	21 (4)
^{50}V					4 (1)	26 (13)
^{49}V					4 (3)	20 (5)
^{48}V					3 (1)	12 (3)
^{50}Ti					1 (1)	
^{48}Ti					3 (1)	6 (3)

signing gamma lines to specific nuclides and, for low intensity peaks, in their area determination. These errors do not include the effects of possible missed transitions to the ground state or the direct feeding of the ground state in the nuclear reaction.

C. Cross sections determined from residual radioactivity

Short (30 m or less) and long (up to 5 h) irradiations of the target stacks were performed. Using well shielded high resolution Ge(Li) detectors, the cross sections of the radioactive products were determined by counting γ-ray spectra from irradiated ^{59}Co targets and associated Al catchers for a period of about three months. The absolute values of the cross sections were obtained from measured peak areas using known total beam charge collected during the irradiation. At 149.5 MeV bombarding energy, where two different Faraday cups were used (see Sec. II A), very close (within less than 5%) absolute values of the cross sections were obtained.

During the preliminary data evaluation it has been found that for some (but not all) $^{4}He+^{59}Co$ reaction products our absolute values of the cross sections were as much as 30% smaller than those quoted by Michel and Brinkmann.[7] In order to check the values of the integrated charge we have determined the cross section for the

TABLE II. Cross sections (in mb) for ^{4}He+^{59}Co reaction products determined from the radioactivity measurements.

Product	E_{lab} (MeV) 20.1	26.8	37.1	39.8	48.8	54.5	60.4	69.5	71.1	81.5	81.8
^{61}Cu	230 (20)	473 (40)		72 (5)		21 (3)		11.4 (10)			6.3 (10)
^{60}Cu				59 (4)							6.4 (10)
^{57}Ni							0.5 (2)		1.0 (4)	2.6 (6)	
^{61}Co				8.4 (2)		2.6 (5)		2.0 (4)			1.7 (3)
^{60}Co			40 (6)		63 (10)		48 (9)		40 (9)	38 (9)	
^{58}Co^{m+g}	34 (6)	183 (15)	173 (10)		103 (10)		179 (10)		282 (15)	284 (15)	
^{57}Co		0.9 (4)	166 (10)		181 (10)		98 (6)		93 (6)	147 (8)	
^{56}Co			0.2 (1)		17 (1)		52 (3)		36.7 (15)	26 (1)	
^{55}Co								2.8 (6)	3.4 (12)	4.6 (4)	4.1 (7)
^{59}Fe					0.5 (2)		2.6 (3)		3.3 (3)	2.9 (3)	
^{52}Fe											
^{56}Mn						3.5 (5)		8.9 (10)			7.4 (10)
^{54}Mn			6.1 (6)		30 (2)		20 (2)		16 (2)	48 (3)	
^{52}Mn^g							0.26 (7)	6.2 (10)	6.8 (4)	15 (1)	12.3 (5)
^{52}Mn^m											
^{51}Cr										8 (1)	
^{48}V										0.18 (5)	

	E_{lab} (MeV) 92.4	93.6	102.9	103.1	113.8	123.9	134.0	138.2	149.5	198.9
^{61}Cu		4.6 (6)	3.2 (6)					1.0 (4)	0.8 (4)	0.2 (1)
^{60}Cu		3.8 (10)						1.2 (6)	0.8 (3)	0.2 (1)
^{57}Ni	4.0 (4)		4.1 (7)	4.3 (6)	4.0 (6)	3.5 (7)	3.5 (7)			2.0 (4)
^{61}Co		1.6 (3)	1.4 (3)					0.7 (1)	0.7 (1)	
^{60}Co	35 (9)			35 (9)	27 (8)	27 (8)	27 (8)		25 (7)	23 (7)
^{58}Co^{m+g}	252 (15)			240 (15)	220 (15)	208 (15)	205 (15)		186 (15)	168 (15)
^{57}Co	180 (8)			177 (8)	159 (8)	149 (10)	146 (10)		133 (10)	106 (10)
^{56}Co	30.2 (8)			40.3 (10)	43.4 (8)	41.0 (12)	40 (2)		38 (1)	32 (2)
^{55}Co		4.0 (10)		3.7 (3)		4.4 (5)	4.8 (1)	4.6 (3)	5.0 (5)	4.5 (6)
^{59}Fe	3.0 (3)			3.0 (3)	2.9 (4)	3.0 (4)	3.1 (5)		2.8 (7)	2.8 (7)
^{52}Fe								0.23 (5)	0.26 (4)	0.37 (3)
^{56}Mn		7.2 (4)	8.0 (12)					9.3 (6)	10 (1)	12 (1)
^{54}Mn	93 (8)			107 (10)	96 (8)	92 (8)	95 (8)		94 (8)	96 (8)
^{52}Mn^g	12.8 (5)	10.8 (10)	10.5 (15)	12.9 (4)	18.4 (5)	26.8 (8)	31.4 (10)	32.2 (15)	32.7 (10)	31 (2)
^{52}Mn^m		1.7 (3)						4.5 (4)	5.2 (4)	

TABLE II. (*Continued*).

	E_{lab} (MeV)																	
	92.4		93.6		102.9		103.1		113.8		123.9		134.0		138.2		149.5		198.9	
^{51}Cr	31	(2)					45	(2)	44	(2)	45	(2)	54	(5)			65	(7)	64	(6)
^{49}Cr															2.3	(4)	2.8	(4)	6.3	(8)
^{48}Cr													0.06	(3)	0.07	(3)	0.14	(4)	0.4	(1)
^{48}V	1.1	(2)					2.8	(3)	3.4	(3)	4.0	(3)	6.0	(4)			11	(1)	19	(1)
^{48}Sc							0.1	(1)			0.11	(6)	0.2	(1)			0.5	(2)		
^{47}Sc							0.3	(1)	0.6	(2)	1.0	(3)	1.2	(5)	1.0	(5)	1.5	(4)	2.7	(2)
^{46}Sc							0.38	(7)	0.6	(2)	1.1	(2)	2.1	(3)			3.3	(3)	6.6	(6)
^{44}Sc^{g}															0.43	(15)	0.40	(15)	2.4	(3)
^{44}Sc^{m}											0.5	(2)	0.6	(2)			0.85	(20)	3.3	(3)

production of ^{22}Na from thin Al catchers and thick beam degraders (including the recoils of ^{22}Na from these catchers and degraders) and compared them with cross sections given in Ref. 19. Figure 1 shows the result of this comparison. The present cross sections are uniformly about 15% lower than those reported in Ref. 19. Although the difference is not as large as in the case of some reaction products in ^{4}He+^{59}Co when compared with data of Ref. 7, it might suggest some overestimation of the total charge measured in our experiment. However, recently Gadioli *et al.*[8] reported absolute values of the cross sections in the ^{4}He+^{59}Co reaction up to 85 MeV bombarding energy, and their data are in excellent agreement with the cross sections measured in the present work. In addition, the cross sections measured by the Köln group[9] for radioactive products in ^{3}He+^{59}Co reaction are, within quoted errors, in good agreement with our data. Therefore no normalization of the present data was attempted.

The cross sections for the radioactive products in the ^{4}He+^{59}Co reaction are listed in Table II and shown in Fig. 2 and those for ^{3}He+^{59}Co are listed in Table III.

D. Recoil ranges of the radioactive reaction products

Thick target recoil ranges R are listed in Tables IV and V for ^{4}He and ^{3}He induced reactions, respectively. They are also displayed in the lower parts of Fig. 2 for the ^{4}He projectile. The thick target recoil ranges are determined[14] from the target thicknesses combined with the measured fraction F of the activity of a given reaction product which recoils out of the target in the forward direction.

From the data given in Tables IV and V we obtain the recoil range values as a function of ΔA, the difference between the compound nucleus mass ($A=62$ and 63 for the ^{3}He and ^{4}He induced reactions, respectively). An example of R vs ΔA plot is shown in Fig. 3 for ^{3}He induced reactions at a bombarding energy of 146 MeV.

In order to obtain information about the linear momenta of the recoiling products, their ranges were converted to velocities parallel to the beam direction ($v_{||}$) with the help of range-energy tables.[20] The correction for the evaporation velocity vector[14] was neglected in the calculation of $v_{||}$. In the recoil range limits which are revelant for this work, the ranges are almost exactly proportional to the recoil velocity.[20] It was shown in Ref. 21 that under these conditions, and with the assumption of an isotropic distribution of the evaporation vector, the evaporation contribution to the thick target recoil ranges may be neglected to the first order. This is in agreement with the experimental data: even for the products most distant from the compound nucleus, the recoil ranges near threshold are equal or lower than the values calculated, assuming full momentum transfer and neglecting correction for evaporation.

The correction to $v_{||}$ arising from the angular distribution of the recoils was also neglected. This correction arises because $v_{||}$ deduced from the stopping distance projected on the beam direction (as measured in this work) is not precisely the same as $v_{||}$ deduced from the projection of the velocity of all recoils. However, using the mea-

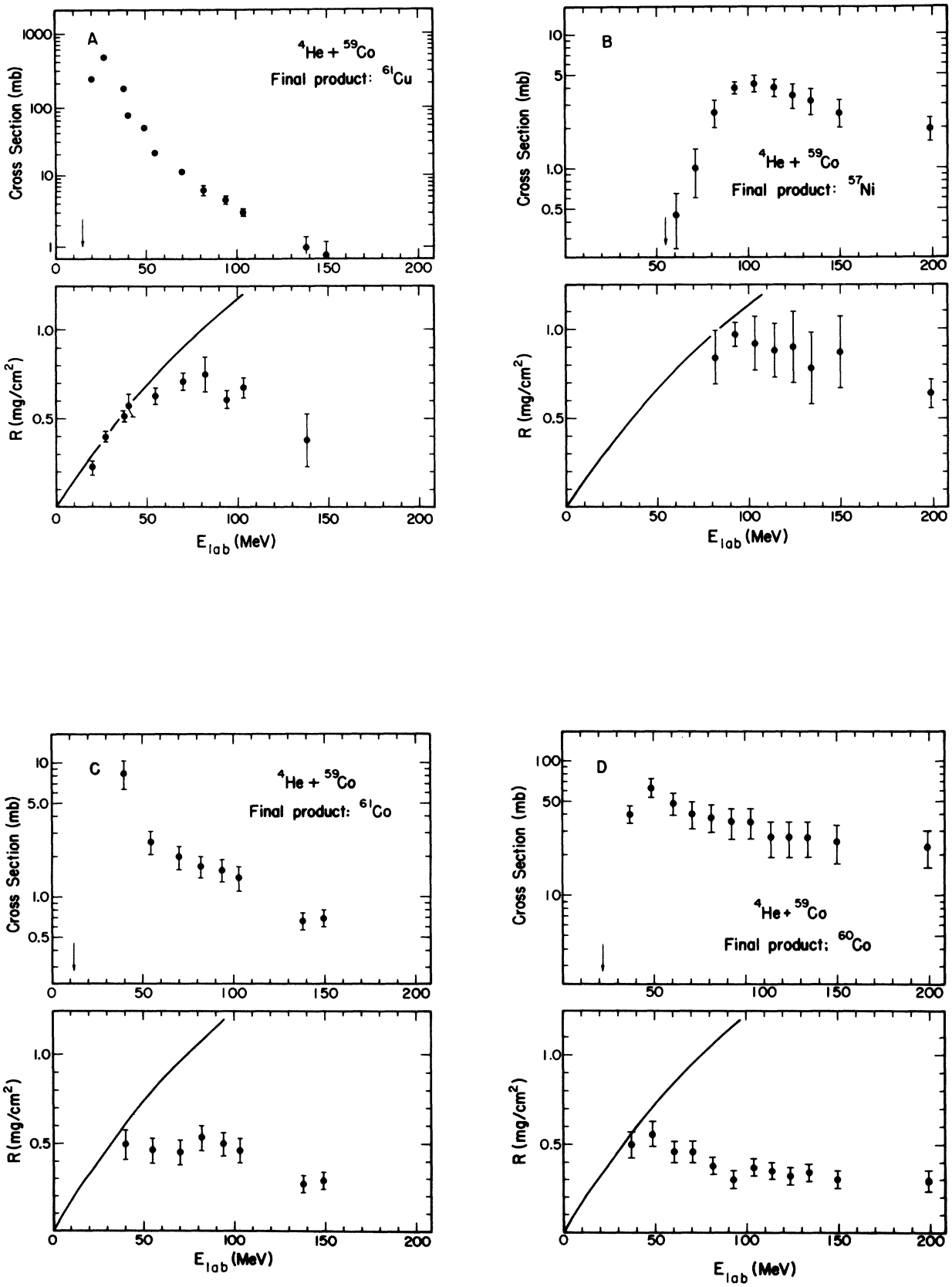

FIG. 2. Cross sections and thick target recoil ranges of the radioactive nuclei produced from ^{4}He bombardment of ^{59}Co target as a function of ^{4}He energy. The curves represent the calculated recoil ranges with the assumption of a full momentum transfer reaction to the compound nucleus. Arrows indicate the energies of the reaction thresholds.

sured angular distribution of recoils (see Sec. II E) and the range-energy relationship,[20] we estimate that this correction is smaller than 10% for the most side-peaking recoils (^{58}Co), and is below 3% for other reaction products.

Figure 4 gives an example of the deduced $v_{||}$ values as a function of ΔA for the ^{4}He induced reactions at a bombarding energy of 134 MeV.

E. Angular distributions of the radioactive recoils

These measurements were performed in a scattering chamber at 81 and 118 MeV α-particle bombarding energy. Small diameter targets of 150 or 200 μg/cm^2 thickness, oriented perpendicular to the beam direction, were irradiated for about 8 h by a ^{4}He^{++} beam of about

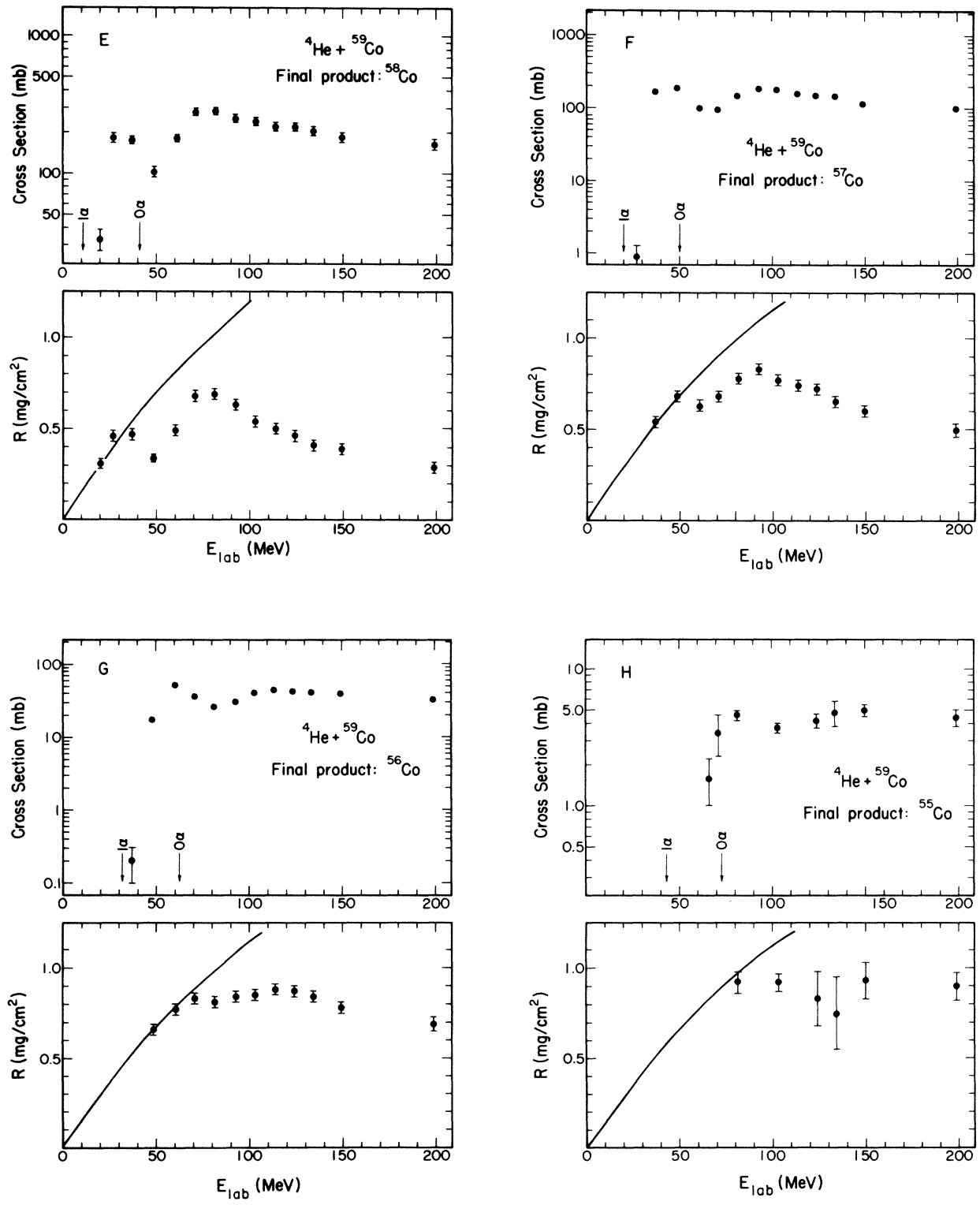

FIG. 2. (*Continued*).

150–200 electron nA intensity. The radioactive recoils were collected on 3 mg/cm^2 thick Al catchers placed on a circular surface perpendicular to the beam direction at a distance of about 20 cm from the target. Examples of the angular distributions for Co isotopes are shown in Fig. 5.

III. DATA REDUCTION AND ANALYSIS

A. Total observed cross section

Table VI summarizes the total observed cross section for ^{4}He energies at which both the in-beam and radioac-

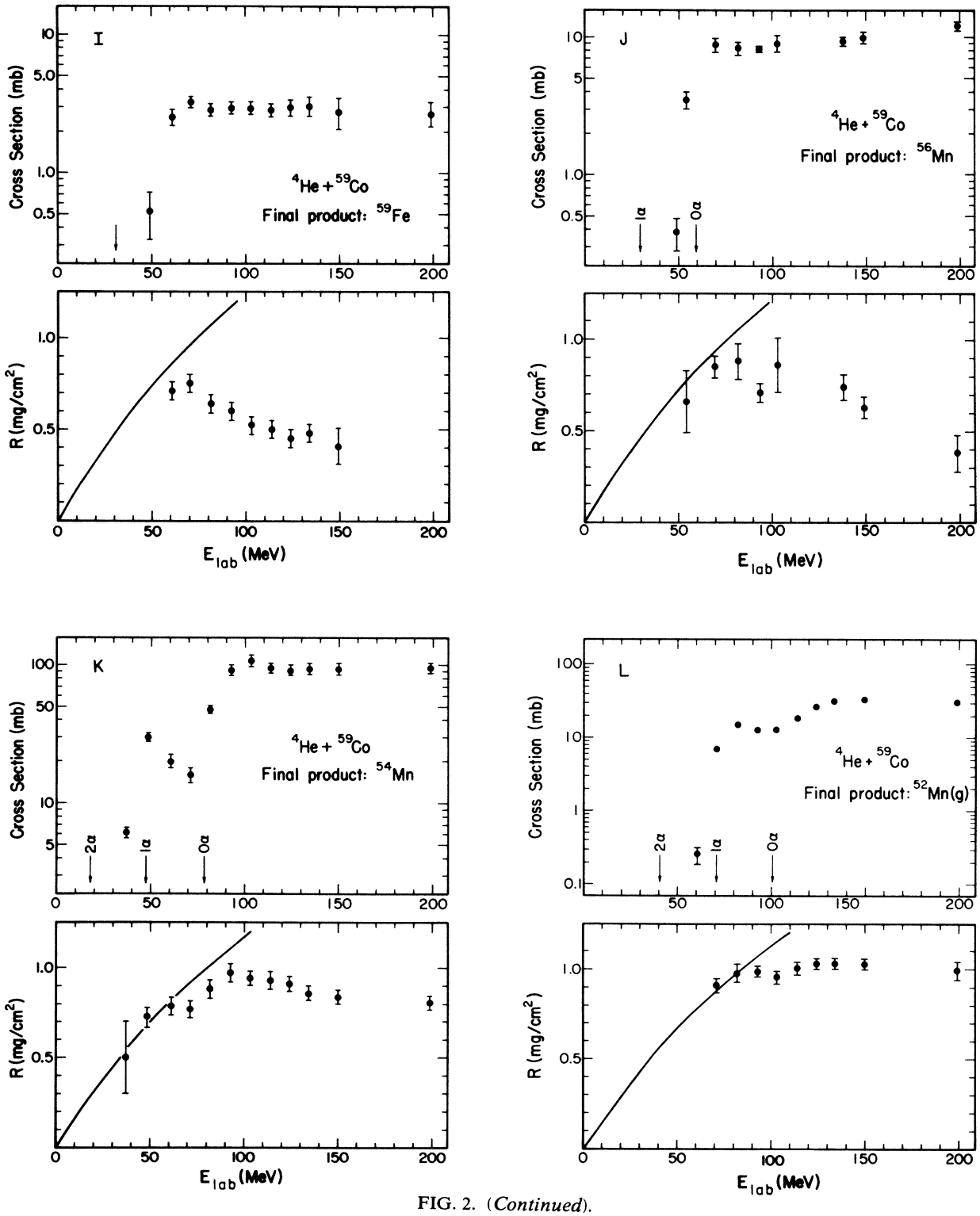

FIG. 2. (*Continued*).

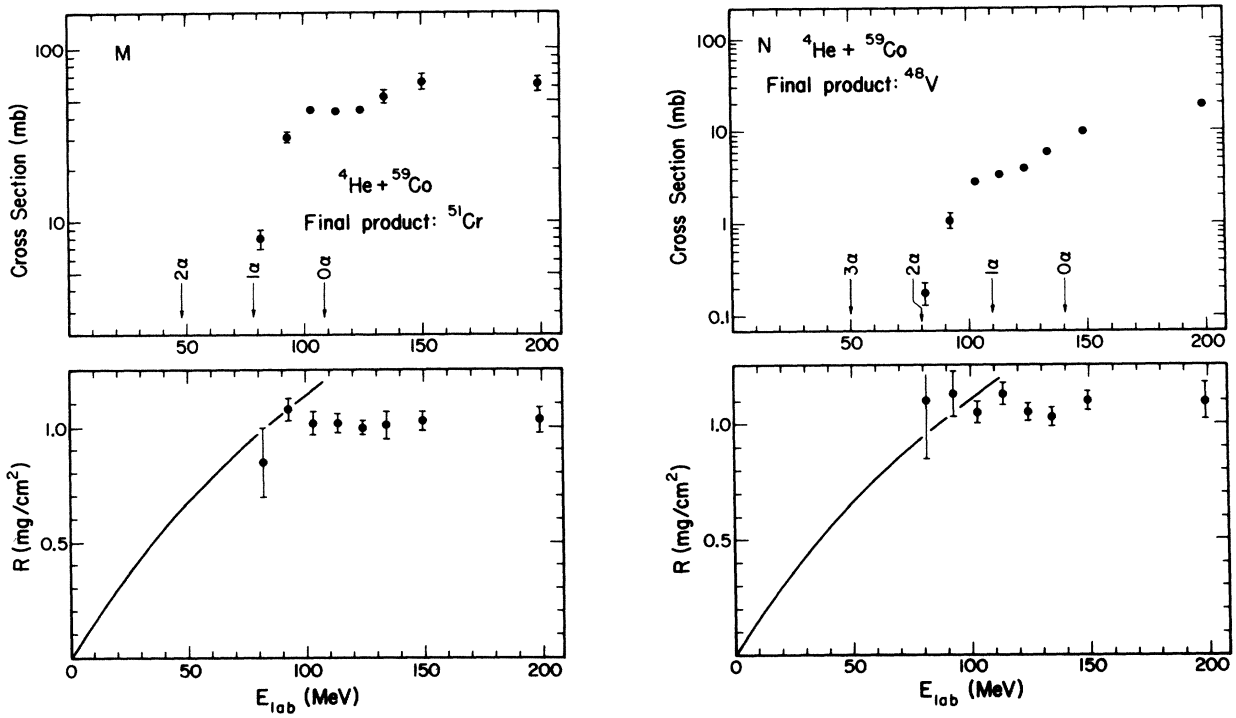

FIG. 2. (*Continued*).

tivity data were obtained. For residual nuclides for which both in-beam and radioactivity data exist the latter cross section value was used. The indicated errors for σ_{obs} take into account the uncertainties assigned to each observed final product (see Sec. II B) but do not include systematic errors which may result from the current integration (up to 15%), target thickness (up to 5%), and the efficiency of the Ge(Li) detectors (±5%). The observed cross section is typically about 90% of the total reaction cross section calculated with the help of the optical model with parameters of Ref. 22.

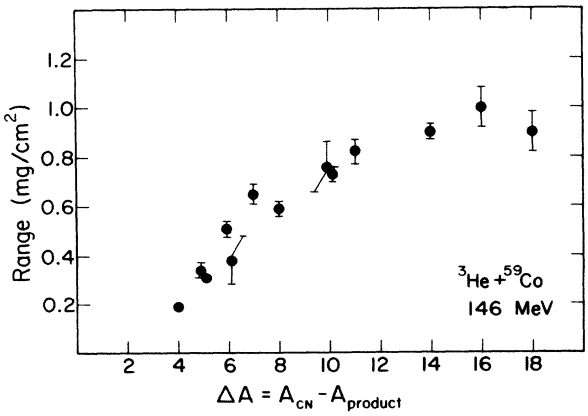

FIG. 3. Thick target recoil ranges of the radioactive products observed in the reaction ^{3}He+^{59}Co at 146 MeV bombarding energy as a function of ΔA, the difference between the hypothetical compound nucleus mass and the mass of the product.

B. Mass and charge distribution

From the cross section data presented in Tables I and II the mass and charge distributions for ^{4}He+^{59}Co residues may be generated. Figure 6 shows these distributions for three representative energies. With increasing bombarding energy both the mass and charge distributions broaden, and at $E_\alpha = 150$ MeV, products of $\Delta A = 18$ are

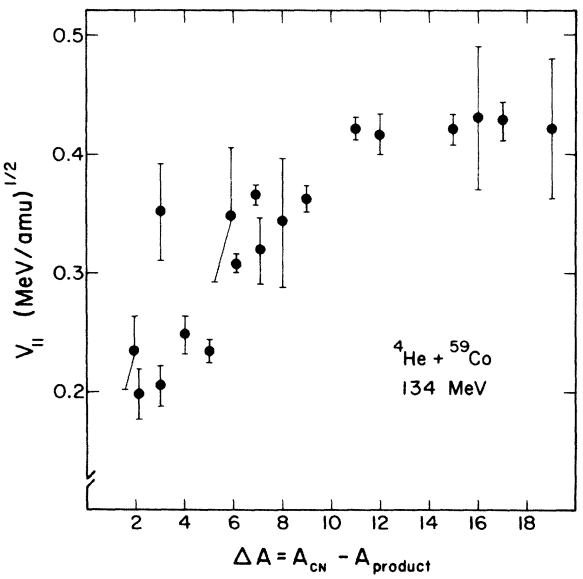

FIG. 4. The recoil velocities projected on the beam direction, deduced from the recoil ranges in the reaction ^{4}He+^{59}Co at 134 MeV bombarding energy, as a function of ΔA.

TABLE III. Cross sections (in mb) for ^{3}He+^{59}Co reaction products determined from the radioactivity measurements.

Product	E_{lab} (MeV) 11	19	32	34	38.1	44.2
^{61}Cu	3.3 (4)	6.1 (5)	2.6 (2)		1.8 (2)	
^{57}Ni				0.03 (2)	0.26 (4)	0.7 (1)
^{60}Co	7.8 (7)	50 (4)	59 (7)	62 (3)	50 (5)	44 (4)
^{58}Co^{m+g}	12 (2)	22 (2)	77 (6)	85 (5)	207 (10)	356 (18)
^{57}Co	15 (2)	72 (2)	41 (2)	34 (2)	32 (2)	46 (3)
^{56}Co	0.4 (1)	1.0 (2)	45 (2)	49 (2)	43 (2)	35 (2)
^{55}Co			0.12 (3)	1.2 (3)	1.4 (2)	4.1 (4)
^{59}Fe		0.15 (9)	1.2 (4)	1.0 (5)	2.0 (3)	
^{52}Fe						
^{56}Mn		0.16 (6)	2.7 (4)		3.2 (4)	
^{54}Mn	a	a	a	a	1.1 (3)	1.6 (3)
^{52}Mn^g				0.14 (6)	0.3 (1)	2.3 (3)
^{51}Cr						
^{48}V						
^{46}Sc						
^{44}Sc^m						

[a] Gamma transition from the decay of ^{54}Mn was inadvertantly lost during the data analysis at these energies.

observed. From the mass and charge distributions the average mass and charge removed from the hypothetical compound nucleus may be obtained. These quantities are discussed in the following section.

In Fig. 7 the mass and charge distributions at approximately the same excitation energy are compared for reactions induced by ^{4}He, ^{6}Li (Ref. 4), and ^{13}C (Ref. 23) ions, all leading to composite systems with $A \simeq 60$. The ^{13}C data present a mass distribution which is less smooth than that of the lighter projectiles. This may be due to a clear separation of nuclei produced in the transfer reactions (dashed blocks in this figure) from the evaporation products in this reaction. In the present work, the methods

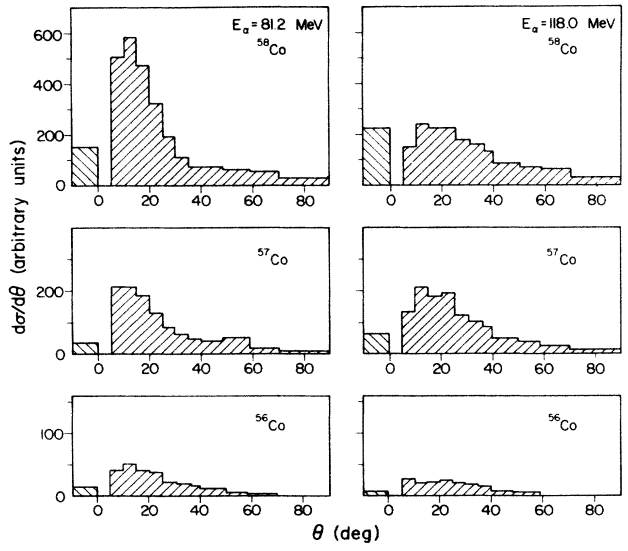

FIG. 5. Angular distributions of the radioactive Co recoils determined at ^{4}He energies of 81 and 118 MeV. Blocks below 0° indicate the activity that remained in the target.

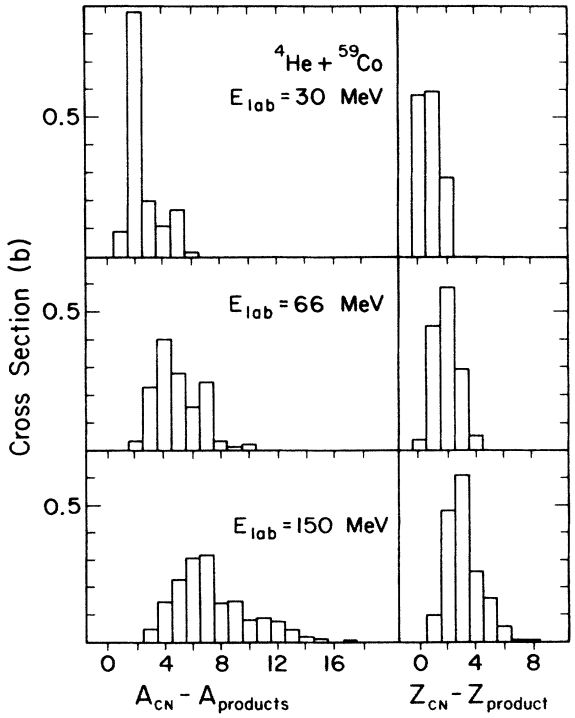

FIG. 6. Mass and charge distributions of the ^{4}He+^{59}Co reaction products at three bombarding energies.

TABLE III. (*Continued*).

E_{lab} (MeV) 55.0		65.5		76.1		96.3		106.3		121.3		146.3	
5.1	(5)	8.9	(7)	8.5	(6)	6.3	(5)	4.6	(5)	4.8	(2)	3.6	(2)
26	(2)	28	(3)	26	(3)	19	(2)			17	(3)		
375	(14)	322	(15)	287	(14)	228	(11)	201	(10)	198	(13)	160	(10)
176	(9)	241	(11)	223	(10)	174	(9)	155	(7)	163	(10)	133	(9)
17	(1)	31	(1)	57	(2)	56	(2)	49	(2)	52	(3)	40	(3)
4.2	(3)	3.2	(3)	3.6	(3)	5.9	(4)	7.0	(4)	6.7	(6)	6.2	(5)
2.0	(3)	1.7	(4)	1.9	(4)	1.9	(3)	1.9	(3)	2.0	(3)	1.6	(5)
										0.4	(1)	0.4	(1)
										6.0	(6)	5.4	(4)
30	(2)	63	(3)	88	(4)	70	(3)	69	(3)	78	(5)	72	(4)
9.0	(3)	6.7	(3)	6.4	(3)	26	(2)	26	(2)	29	(2)	29	(2)
4.3	(2)	26	(2)	32	(3)	27	(2)	42	(3)	54	(3)	58	(3)
0.04	(2)	0.6	(1)	1.6	(2)	2.1	(1)	3.7	(2)	8.7	(8)	12	(1)
								1.0	(1)	1.7	(4)	2.3	(4)
						0.3	(1)	0.4	(1)	0.6	(2)	1.4	(2)

employed did not separate transfer reaction products from the evaporation residues for He induced reactions.

C. Average removed mass and charge

The average, cross-section-weighted removed mass $\overline{\Delta A}$ is shown in Fig. 8 for ^{4}He+^{59}Co as a function of the projectile energy. In the same figure we present also $\overline{\Delta A}$ for p+^{62}Ni (Ref. 2), ^{6}Li+^{56}Fe (Ref. 4), and ^{13}C+Ti (Ref. 23) reactions. The values of $\overline{\Delta A}$ for the ^{13}C reaction on different Ti isotopes evaluated from Ref. 23 data are independent of target neutron number N. This is in agreement with results of Ref. 24, which also show that in the mass region around $A=150$, $\overline{\Delta A}$ is independent of N for a large range of excitation energies.

At low α-particle bombarding energies, up to about 10

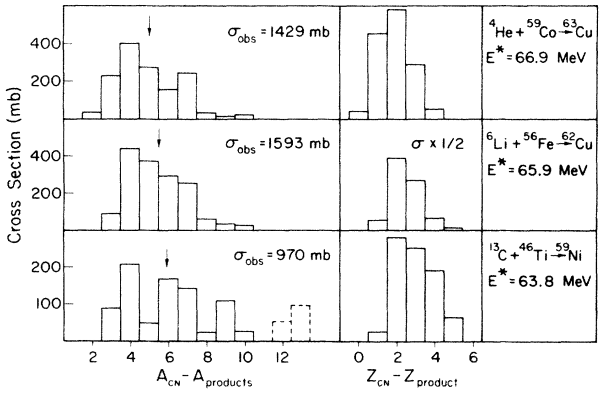

FIG. 7. Comparison of mass and charge distributions for ^{4}He+^{59}Co, ^{6}Li+^{56}Fe, and ^{13}C+^{46}Ti reactions at similar excitation energy of the compound system. ^{13}C data are from Ref. 23. Arrows indicate the calculated average removed mass $\overline{\Delta A}$ (also see Fig. 8). The dashed blocks for the ^{13}C+^{46}Ti reaction account for observed transfer reactions (products close to the target) and were not taken into account in the calculation of the average removed mass.

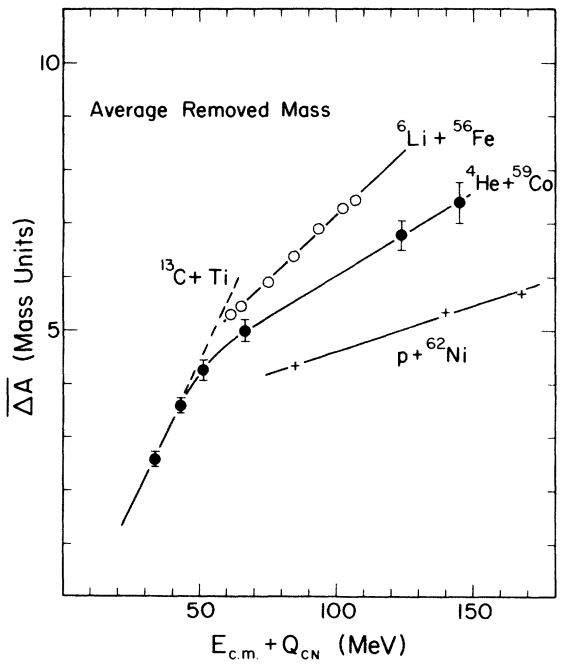

FIG. 8. Average removed mass $\overline{\Delta A}$ from the hypothetical compound nucleus as a function of $E_{c.m.}+Q_{CN}$ ($=E^*$ in the case of the formation of the compound nucleus) for p+^{62}Ni (Ref. 2), ^{4}He+^{59}Co, ^{6}Li+^{56}Fe (Ref. 4), and ^{13}C+Ti reaction. The dashed line in this figure is a fitted line to all $\overline{\Delta A}$ values deduced from Ref. 23 data. Other lines are to guide the eye only.

TABLE IV. Thick target recoil ranges (in mg/cm^2 in Co) for ^{4}He+^{59}Co reaction products.

Product	E_{lab} (MeV) 20.1	26.8	37.1	39.8	48.8	54.5	60.4	69.5	71.1	81.5	81.8
^{61}Cu	0.2 (4)	0.40 (3)		0.57 (6)		0.63 (5)		0.71 (5)			0.75 (10)
^{60}Cu				0.62 (6)							0.81 (15)
^{57}Ni										0.84 (15)	
^{61}Co				0.49 (8)		0.46 (8)		0.45 (8)			0.53 (8)
^{60}Co			0.50 (7)		0.56 (7)		0.46 (6)		0.46 (6)	0.38 (5)	
^{58}Co^{m+g}	0.31 (3)	0.47 (3)	0.47 (3)		0.34 (2)		0.49 (3)		0.68 (3)	0.69 (3)	
^{57}Co			0.54 (3)		0.68 (3)		0.63 (3)		0.68 (3)	0.78 (3)	
^{56}Co					0.66 (3)		0.77 (3)		0.83 (3)	0.81 (3)	
^{55}Co								0.83 (6)		0.92 (6)	1.07 (10)
^{59}Fe							0.71 (5)		0.75 (5)	0.64 (5)	
^{52}Fe											
^{56}Mn						0.66 (17)		0.85 (6)			0.88 (10)
^{54}Mn			0.5 (2)		0.73 (6)		0.79 (5)		0.77 (5)	0.88 (5)	
^{52}Mn^g								0.82 (10)	0.91 (4)	0.98 (5)	1.09 (6)
^{51}Cr										0.85 (15)	
^{48}V										1.10 (25)	

	E_{lab} (MeV) 92.4	93.6	102.9	103.1	113.8	123.9	134.0	138.2	149.5	198.9
^{61}Cu		0.61 (5)	0.68 (6)					0.38 (15)		
^{60}Cu		0.50 (10)						0.68 (35)	0.89 (20)	
^{57}Ni	0.97 (7)			0.92 (15)	0.88 (15)	0.9 (2)	0.78 (20)		0.87 (15)	0.64 (8)
^{61}Co		0.50 (8)	0.46 (7)					0.37 (5)	0.31 (5)	
^{60}Co	0.30 (5)			0.37 (5)	0.35 (5)	0.32 (15)	0.34 (5)		0.30 (5)	0.29 (6)
^{58}Co^{m+g}	0.63 (3)			0.54 (3)	0.50 (3)	0.46 (3)	0.41 (3)		0.39 (3)	0.29 (3)
^{57}Co	0.83 (2)			0.77 (3)	0.74 (2)	0.71 (3)	0.65 (3)		0.60 (3)	0.50 (4)
^{56}Co	0.84 (3)			0.85 (4)	0.88 (4)	0.87 (3)	0.84 (3)		0.78 (4)	0.69 (4)
^{55}Co		0.67 (15)		0.92 (5)		0.83 (15)	0.75 (20)	0.99 (4)	0.96 (6)	0.90 (7)
^{59}Fe	0.60 (5)			0.52 (7)	0.50 (5)	0.45 (5)	0.48 (5)		0.41 (10)	
^{52}Fe								1.19 (10)	1.05 (15)	0.98 (5)
^{56}Mn		0.71 (5)	0.86 (15)					0.74 (7)	0.63 (6)	0.38 (10)
^{54}Mn	0.97 (5)			0.94 (4)	0.93 (3)	0.91 (4)	0.85 (4)		0.84 (5)	0.81 (4)
^{52}Mn^g	0.99 (3)	1.02 (12)	0.94 (13)	0.96 (3)	1.01 (3)	1.03 (3)	1.03 (3)	1.06 (8)	1.03 (3)	0.99 (5)
^{51}Cr	1.08 (5)			1.02 (5)	1.02 (4)	1.00 (3)	1.01 (6)		1.03 (4)	1.03 (5)
^{49}Cr								1.12 (6)	1.04 (6)	

TABLE IV. (*Continued*).

	E_{lab} (MeV)																			
	92.4		93.6		102.9		103.1		113.8		123.9		134.0		138.2		149.5		198.9	
^{48}Cr													1.0	(3)	1.0	(3)	1.06	(15)	0.99	(13)
^{48}V	1.13	(10)					1.05	(5)	1.13	(5)	1.05	(4)	1.03	(4)			1.10	(4)	1.10	(8)
^{47}Sc							1.25	(25)	1.1	(2)	1.15	(20)	1.1	(2)			1.05	(10)		
^{46}Sc							1.13	(15)	1.3	(1)	1.35	(10)	1.06	(5)			1.14	(4)	1.14	(10)
^{44}Sc^{m}											1.15	(20)	1.0	(2)						

MeV/nucleon, Fig. 8 shows that as energy increases, $\overline{\Delta A}$ increases linearly with a slope of 1 nucleon/9.3 MeV. Extrapolation of the $\overline{\Delta A}$ curve down to $\overline{\Delta A}=0$ suggests a threshold of about 8 MeV, consistent with the value of the separation energy of the last nucleon from the compound system.

At an excitation energy of about 50 MeV the $\overline{\Delta A}$ curve for the $\alpha+$Co reaction changes its slope to a value of 1 nucleon/32 MeV (see Fig. 8), clearly indicating the onset of nonequilibrium processes at this energy. At the same excitation energy the heavy ion (^{13}C+Ti) data do not exhibit a similarly pronounced bend. This comparison, together with that of the p, ^{4}He, and ^{6}Li results in Fig. 8, indicates a progressive increase (for a given excitation energy) in the yield of the nonequilibrium processes as the mass of the projectile decreases. (The relation of the average removed mass to the energy deposition will be discussed in Sec. II F.)

In contrast to $\overline{\Delta A}$, the average removed charge $\overline{\Delta Z}$ depends critically on the distance of the compound nucleus from the beta stability line.[24] Figure 9 shows the $\overline{\Delta Z}$ values for ^{4}He+^{59}Co and p+^{62}Ni reactions, for which the composite system is the same. The ^{13}C+Ti data[23] are shown for ^{46}Ti and ^{47}Ti targets. The ^{63}Cu* nucleus formed in ^{4}He and p induced reactions has a displacement from the beta stability line [defined as $(N/Z)_{stab}-(N/Z)_{CN}$, where $(N/Z)_{stab}$ is calculated for even-even, abundancy-weighted stable isotopes of a given element and CN denotes composite nucleus] intermediate between ^{59}Ni* and ^{60}Ni* nuclei formed with ^{13}C ions on ^{46}Ti and ^{47}Ti targets, respectively.

The onset of nonequilibrium processes in $\alpha+$Co reactions at an energy of about 10 MeV/nucleon is also clearly seen in the $\overline{\Delta Z}$ dependence on bombarding energy (Fig. 9). As for the $\overline{\Delta A}$ dependence, the extrapolation of the $\overline{\Delta Z}$ curve to $\overline{\Delta Z}=0$ now shows a threshold of about 20 MeV.

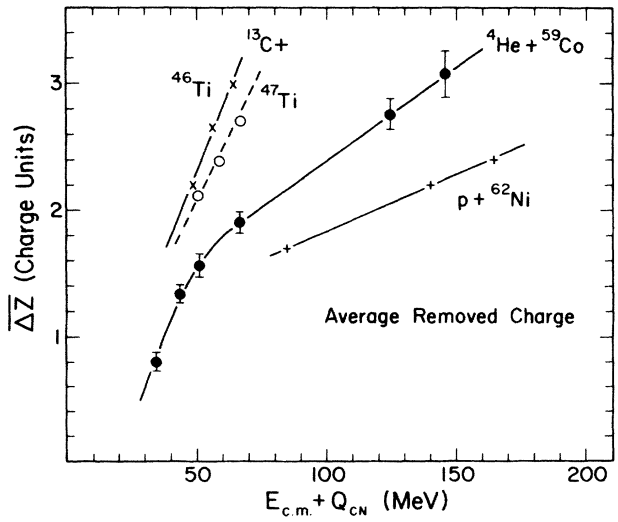

FIG. 9. Average removed charge $\overline{\Delta Z}$ from the hypothetical compound nucleus as a function of $E_{c.m.}+Q_{CN}$. Also see caption to Fig. 8.

TABLE V. Thick target recoil ranges (in mg/cm^2 in Co) for ^{3}He+^{59}Co reaction products.

Product	E_{lab} (MeV) 11	19	32	34	38.1	44.2
^{57}Ni						0.25 (5)
^{60}Co		0.18 (4)	0.28 (9)	0.17 (5)	0.22 (8)	0.17 (5)
^{58}Co^{m+g}	0.14 (2)	0.14 (2)	0.24 (2)	0.28 (2)	0.32 (2)	0.39 (3)
^{57}Co	0.28 (4)	0.33 (4)	0.38 (3)	0.33 (3)	0.27 (2)	0.33 (3)
^{56}Co	0.34 (2)	0.23 (4)	0.47 (4)	0.45 (4)	0.46 (4)	0.48 (3)
^{55}Co					0.55 (10)	0.48 (5)
^{52}Fe						
^{56}Mn					0.51 (15)	
^{54}Mn					0.36 (16)	0.47 (10)
^{52}Mn^g					0.30 (12)	0.54 (4)
^{51}Cr						
^{48}V						
^{46}Sc						
^{44}Sc^m						

It is unlikely that the whole 12 MeV difference between $\overline{\Delta A}$ and $\overline{\Delta Z}$ thresholds is due to Coulomb barrier effects in the α-evaporation process. One possible explanation of this observation may come from the fact that Γ_{CP}/Γ_n, the ratio of charged particle emission width to the neutron emission width, increases with increasing angular momentum of the decaying nucleus. This increase is particularly fast for α-particle emission. Lower energy α-particle data[25] are necessary in order to investigate the difference in threshold values with more precision and to test the relevance of charged particle emission from high-l space.

D. Recoil velocities of individual reaction products

Figures 10–12 show the deduced average recoil velocities (in compound nucleus velocity units) of the individual final products of the ^{4}He+Co reactions as a function of the bombarding energy above the threshold of each reaction channel. Close to the threshold these velocities are equal to or slightly lower than compound nucleus velocities. When the bombarding energy increases, substantial differences between various products appear, indicating, in agreement with the finding of Ref. 8, that a variety of reaction mechanisms is effective in the production of final nuclei in ^{4}He+^{59}Co reactions.

A pronounced dip in ^{58}Co velocities and less pronounced minima for ^{57}Co, ^{56}Co, and ^{54}Mn are observed at 30–50 MeV above threshold. A similar pattern of the recoil velocities for analogous reaction channels is also found in ^{6}Li- and ^{3}He-induced reactions at approximately the same bombarding energy above threshold. These minima may be interpreted as evidence for preequilibrium α-particle emission.[8]

E. Average and maximum linear momentum transfer

The thick target recoil ranges determined in the present work were used to deduce the average and maximum LMT from ^{3}He and ^{4}He projectiles to the heavy reaction residues. The general outlook on LMT in nuclear reactions, references to other methods and results, as well as our data for the ^{4}He+^{59}Co reactions have been presented in an earlier paper.[6] Here we present some supplementary details about the general method of extracting the average and maximum momentum transfer from the recoil range data.

For many years the measurements of recoil ranges of radioactive nuclei have been a rich source of information about the transferred linear momentum.[14,26,27] The conclusions from these measurements were, however, limited to reaction channels leading to radioactive final products, which always represent only a fraction of all reaction

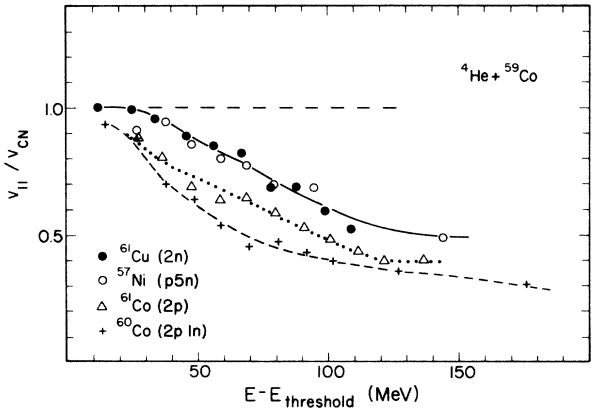

FIG. 10. Forward mean velocities (in compound nucleus velocity units $v_{||}/v_{CN}$) of ^{61}Cu, ^{57}Ni, ^{61}Co, and ^{60}Co final products observed for ^{4}He+^{59}Co as a function of the bombarding energy above the threshold of the given reaction channel. The reaction channel is identified in the figure in parentheses after the product label. The lines are to guide the eye.

TABLE V. (*Continued*).

E_{lab} (MeV) 55.0	65.5	76.1	96.3	106.3	121.3	146.3
0.51 (9)	0.59 (9)	0.64 (7)	0.52 (5)	0.53 (5)	0.43 (4)	0.34 (3)
0.20 (5)	0.13 (5)	0.26 (5)	0.37 (5)		0.47 (7)	
0.41 (3)	0.36 (3)	0.32 (3)	0.27 (3)	0.26 (3)	0.21 (2)	0.19 (2)
0.49 (4)	0.53 (3)	0.52 (3)	0.45 (4)	0.44 (3)	0.35 (2)	0.31 (2)
0.48 (3)	0.52 (3)	0.63 (3)	0.63 (3)	0.63 (3)	0.51 (2)	0.51 (3)
0.55 (6)		0.68 (5)		0.67 (4)	0.62 (4)	0.65 (4)
					0.64 (7)	0.76 (10)
					0.60 (20)	0.38 (10)
0.55 (4)	0.62 (4)	0.66 (4)	0.63 (5)	0.71 (4)	0.62 (3)	0.59 (3)
0.63 (3)	0.71 (3)	0.68 (2)	0.79 (3)	0.78 (3)	0.77 (2)	0.73 (3)
	0.68 (4)	0.69 (3)	0.77 (4)	0.69 (5)	0.81 (4)	0.82 (5)
	0.73 (8)	0.74 (5)	0.78 (4)	0.87 (3)	0.91 (4)	0.90 (3)
				1.12 (12)	0.99 (5)	1.00 (8)
			0.78 (4)	0.89 (15)	1.01 (14)	0.90 (8)

products. To our best knowledge recoil range data have never before been compared with the results of other techniques determining the LMT, such as measurements of the angular correlation between fission fragments for highly fissile elements (see, e.g., Refs. 10 and 11, and references quoted therein) or direct measurements of the recoil velocity by the time of flight method.[28,29]

The systematics of the average momentum transfer for light projectiles acquired by Saint-Laurent *et al.*[10] and the discovery of the limitation of the transferred momentum in heavy ion induced reactions by Galin *et al.*[30] have prompted us to extract from our recoil range data LMT values that may be compared with the results obtained using other methods. In extracting the average momentum transfer we note, by comparing the in-beam and radioactivity data for ^{4}He+^{59}Co, that at all bombarding energies the radioactive nuclei represent about 45% of all observed reaction products and account for about 35% (see Table VI) of the total observed cross section. Therefore it is postulated that radioactive nuclei form a representative sample of all reaction products, and the average values of observables determined for this sample should be close to the average values for the whole population of produced residues. In order to check the assumption that in this mass region the radioactive nuclei form an unbiased sample, we calculated, using the data of Ref. 4, average momentum transfer for ^{6}Li induced reactions[4] on two targets: ^{54}Fe and ^{56}Fe. In this case the same radioactive species will correspond to different ΔA. The results do not show any clear target dependence, although the populations of radioactive nuclei produced in these two reactions are obviously different.

In order to estimate the statistical confidence level at which the average of the radioactive sample approximates the average of the whole population (neglecting the possibility of a systematic bias), it was assumed that the vari-

TABLE VI. Summary of the cross section data for ^{4}He+^{59}Co reaction.

E_{lab} (MeV)	σ_{obs} [a]	$\frac{\sigma_{in\,beam}}{\sigma_{obs}}$ [b]	$\frac{\sigma_{rad}}{\sigma_{obs}}$ [c]	$\overline{\Delta A}$ [d]	$\overline{\Delta Z}$ [e]
30.3	1471 (90)	0.92		2.62 (23)	0.80 (8)
39.8	1635 (61)	0.87	0.36	3.63 (19)	1.34 (7)
49.0	1604 (67)	0.89	0.30	4.18 (25)	1.56 (10)
65.7	1429 (43)	0.85	0.32	4.97 (21)	1.91 (8)
127.3	1263 (36)	0.73	0.49	6.80 (29)	2.76 (12)
149.3	1682 (60)	0.85	0.37	7.37 (39)	3.07 (18)

[a]Total observed cross section for the production of heavy reaction residues from the in-beam and radioactivity measurements.
[b]Fraction of the total observed cross section detected by the in-beam measurements.
[c]Fraction of the total observed cross section detected by the residual radioactivity measurements.
[d]Average removed mass (see Sec. III C).
[e]Average removed charge (see Sec. III C).

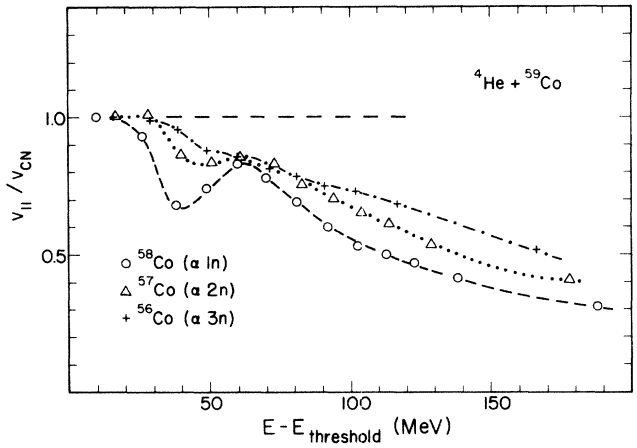

FIG. 11. The same as for Fig. 10 but for ^{58}Co, ^{57}Co, and ^{56}Co final products.

ances $(\overline{p_{||}^2} - \bar{p}_{||}^2)$ of these two populations are the same. With this assumption and knowledge of the number of radioactive and stable products, the 96% confidence level was calculated from the standard formula for the variance of the average value of the sample and normal distribution integrals.

Figures 13 and 14 present the average cross-section-weighted values of the transferred momentum $\langle p_{||} \rangle$ for the radioactive nuclei for ^{4}He- and ^{3}He-induced reactions, respectively. We obtain $\langle p_{||} \rangle$ from $\langle v_{||} \rangle$ simply by multiplying $\langle v_{||} \rangle$ by the mass of the compound nucleus. This facilitates comparison with the full momentum transfer expected for complete fusion processes. For the ^{4}He projectile the error bars indicated in Fig. 13 for $\langle p_{||} \rangle$ correspond to the 96% confidence level discussed above. Errors originating from range and cross section uncertainties are much smaller. As the total number of populated nuclides in the case of the ^{3}He-induced reactions is unknown (no in-beam data were obtained for this reaction), a ±5% error has been assumed for $\langle p_{||} \rangle$ in Fig. 14.

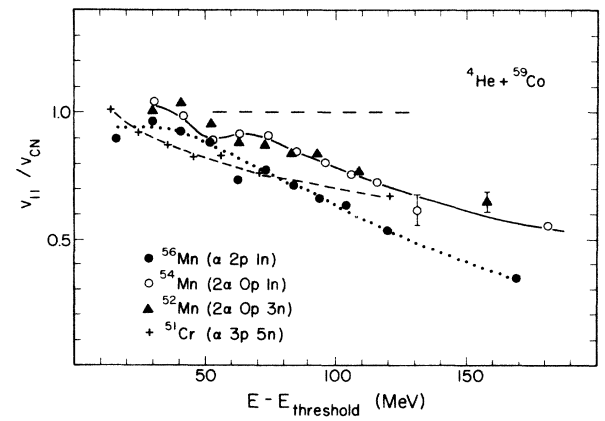

FIG. 12. The same as Fig. 10 but for ^{56}Mn, ^{54}Mn, ^{52}Mn, and ^{51}Cr final products.

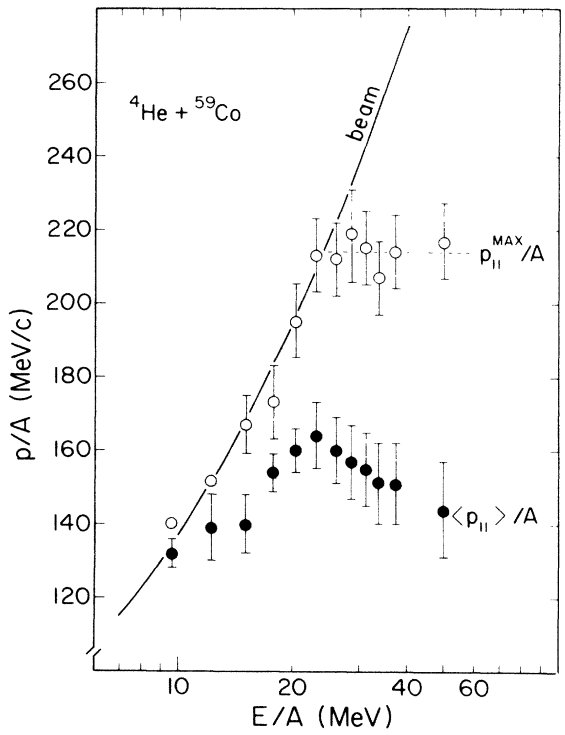

FIG. 13. The average (solid circles) and maximum (open circles) LMT divided by A, the mass of the projectile as a function of the bombarding energy divided by A for the ^{4}He+^{59}Co reaction. The error bars indicated for $\langle p_{||} \rangle$ represent a 96% confidence level (see text). The error bars for $p_{||}^{max}$ reflect the spread of measured velocities for products far removed from the target mass (see Fig. 4).

Another quantity which may be deduced from the recoil range data is the "maximum value" of the transferred momentum, $p_{||}^{max}$. The data presented in Figs. 3 and 4 show that for a given bombarding energy average recoil ranges or recoil velocities projected on the beam direction $\langle v_{||} \rangle$ level off as a function of ΔA for products far removed from the target. Similar behavior of $\langle v_{||} \rangle$ is observed at all bombarding energies employed in this work. The maximum value of the transferred momentum (indicated in Figs. 13 and 14 as open circles) is deduced from the velocities of the products in this saturation region, assuming that the mass of the recoiling nucleus is equal to that of the composite nucleus prior to particle emission.

Evidently it is possible that the reaction products which have even larger ΔA than those observed here may have higher recoil velocities. However, based on the determined mass distribution (see Fig. 6) their total cross section is small and has been estimated to be less than 3% of the observed cross section. It is with this qualification that we define the maximum momentum transfer $p_{||}^{max}$ for ^{3}He- and ^{4}He-induced reactions.

A comment about the operational definition of $p_{||}^{max}$ should be made here. Each recoil range entry in Tables IV and V is evidently an average value by itself. Therefore, $p_{||}^{max}$ in Figs. 14 and 15 is the maximum value of this

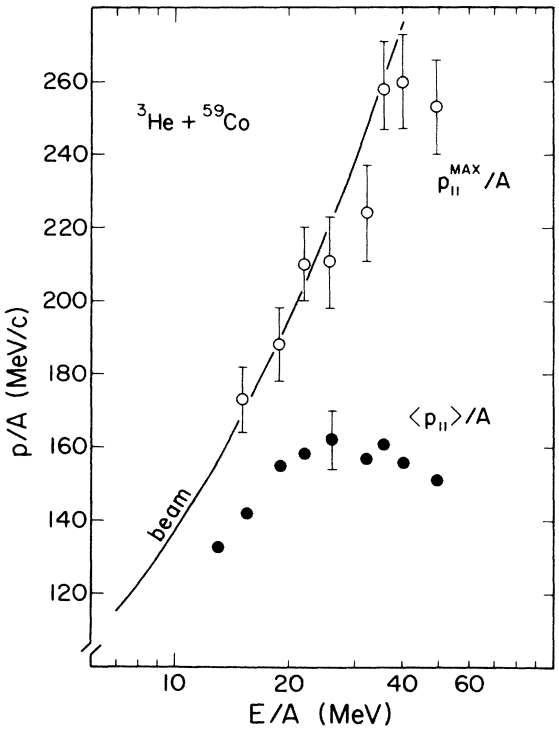

FIG. 14. The same as Fig. 13 but for a ^{3}He projectile. A ±5% error is assumed for $\langle p_{||}\rangle$ (see text).

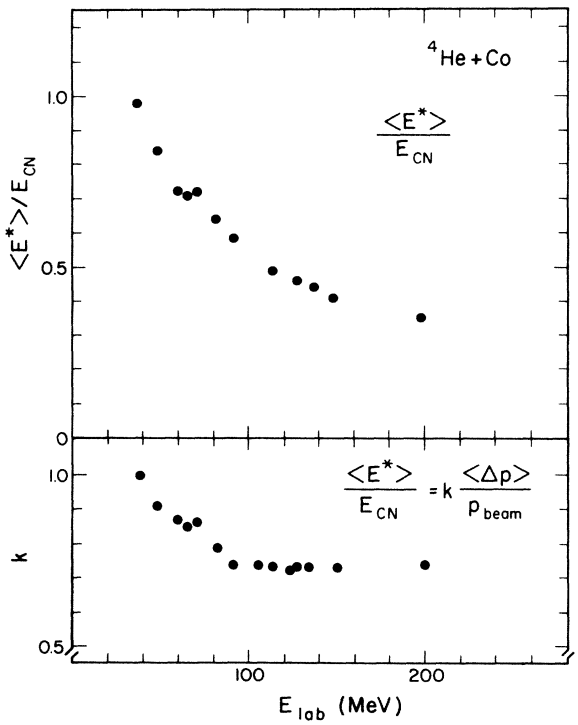

FIG. 15. Upper part: the average excitation energy of the thermalized system (in compound nucleus energy units) in ^{4}He+^{59}Co reaction as a function of ^{4}He bombarding energy. The values of the average removed mass, necessary for the calculation of $\langle E^*\rangle$, were obtained through interpolation and extrapolation of the data presented in Fig. 8. Lower part: the proportionality factor k relating average excitation energy (in compound nucleus energy units) with average transferred linear momentum (in beam momentum units) as a function of ^{4}He bombarding energy.

average and not the maximum allowed transferred momentum in a given nuclear reaction. Thin-target, differential recoil ranges[4,31] could yield more precise information about the "true" maximum momentum transfer. Such measurements are presently in progress.[25]

F. Average energy deposition

While the average transferred linear momentum is measured directly in this work via the recoil ranges, one must introduce additional assumptions about the interaction mechanism in order to obtain from the data information about the average energy deposition (i.e., the excitation energy of the thermalized system remaining after the fast, nonequilibrium reaction phase). We show below that the results inferred depend strongly on the assumptions made.

Let us first use the experimentally determined average removed *mass* to deduce the average excitation energy, E^*, or excitation energy per nucleon, ϵ^*, of the thermalized composite system. From the slope of the dependence of the average removed mass $\overline{\Delta A}$ on the compound nucleus excitation energy at low bombarding energies (Fig. 8), one deduces that the excited nucleus evaporates one nucleon at the expense of about 9.3 MeV excitation energy. In what follows, we assume that this value is independent of excitation energy in the energy range of interest here. In order to convert the experimentally measured $\overline{\Delta A}$ values to effective excitation energies, one needs to know the average mass of the equilibrated emitting system. This mass is calculated under the further assumption that the net (after fast reaction phase) average number of nucleons captured by the target $\overline{\Delta A}_{tr}$ is proportional to the average transferred linear momentum $\langle p_{||}\rangle$,

$$\frac{\overline{\Delta A}_{tr}}{A} = \kappa \frac{\langle p_{||}\rangle}{p_{beam}} , \tag{1}$$

where A and p_{beam} are mass number and momentum of the projectile, respectively, and $\kappa = 1$. (This assumption is evidently an approximation. It implies, for example, that fast nucleons are emitted, on the average, with momentum corresponding to the beam velocity. This effect is supported by theoretical considerations in Ref. 32.)

Under the above assumptions, we extract the effective excitation energy $\langle E^*\rangle$ of the evaporating nucleus by equating the total average removed mass with the sum of the mass removed in the fast stage and that removed by evaporation:

$$\begin{aligned}\overline{\Delta A} &= (A - \overline{\Delta A}_{tr}) + \langle E^*\rangle/9.3 \\ &= A\left[1 - \frac{\langle p_{||}\rangle}{p_{beam}}\right] + \langle E^*\rangle/9.3 .\end{aligned} \tag{2}$$

Combining the data presented in Secs. III C and III E on $\overline{\Delta A}$ and $\langle p_{||}\rangle$, one obtains the average excitation ener-

gy of the thermalized system in compound nucleus energy units shown in the upper part of Fig. 15. The change in slope of $\overline{\Delta A}$ versus bombarding energy shown in Fig. 8 is the manifestation of the substantial decrease in the energy transfer. Above about 70 MeV bombarding energy, an increase in ^{4}He energy by 10 MeV leads only to a 1.5 MeV increase in the average excitation energy of the thermalized system. Similar arguments applied to the ^{6}Li data of Fig. 8 (and taking into account the average linear momentum transfer in this reaction) show that in the investigated ^{6}Li energy range as much as 4 MeV from each 10 MeV bombarding energy is converted, on the average, to excitation energy in the thermalized system.

In a number of previous works (see, e.g., Refs. 33–35) dealing with measurements of the recoil velocities of radioactive products formed in proton and heavier-ion induced reactions, the LMT and excitation energy of the thermalized system were assumed to be related:[36]

$$\frac{E^*}{E_{\mathrm{CN}}} = k\frac{\langle p_{\|}\rangle}{p_{\mathrm{beam}}} \tag{3}$$

(where E_{CN} denotes the excitation energy of the compound nucleus formed by complete fusion of the target and projectile, and $\langle p_{\|}\rangle$ is the transferred linear momentum). The proportionality factor k was often assumed to be in the 0.7–0.8 range, based on results of intranuclear cascade calculations[36,37] for proton induced reactions.

In the current work the factor k in the above relation can be determined from the measurement under the assumptions discussed previously, and obtained results for the value of k are shown in the lower part of Fig. 15. In the ^{4}He bombarding energy range from 90 to 200 MeV, k is indeed constant and equal to 0.73 ± 0.02. Below 90 MeV k increases, reflecting the fact that when the average momentum transfer is equal to the beam momentum, the excitation energy should be equal to the energy of the compound nucleus.

In an alternative approach to the deduction of the excitation energy one can assume, instead of the validity of Eq. (1) with $\kappa=1$, that the proportionality factor k in Eq. (3) is energy independent and equal to 1. (This assumption is equivalent to that proposed in Ref. 38.) The results obtained with $k=1$ are compared to those with $\kappa=1$ in Fig. 16. As was to be expected from the energy dependence of k presented in Fig. 15, the two approaches give quite different excitation energies, as shown in Fig. 16. These differences indicate that the fractional energy, linear momentum, and mass transfers are not all equal for ^{4}He-induced reactions in the energy range discussed here. An equality of all three quantities would be expected in the limit in which mass, energy, and momentum are all removed from the composite system solely by the emission of fast forward-going nucleons with the beam velocity. Our results thus show that this limit is not applicable to the system studied at the higher bombarding energies. Independent measurements (e.g., of evaporated particle multiplicities) sensitive directly to the temperature of the thermalized system would provide additional constraints on the ^{4}He+Co interaction mechanism.

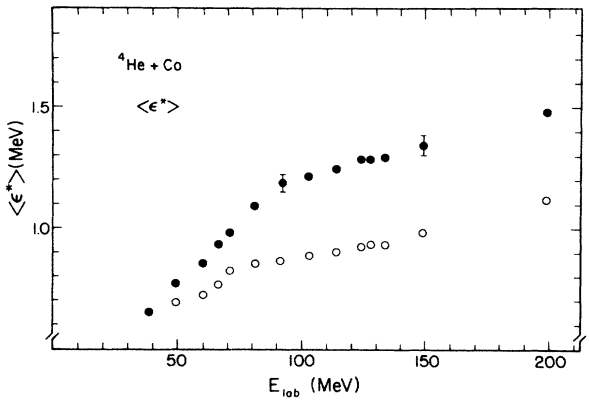

FIG. 16. Average excitation energy per nucleon in the ^{4}He+^{59}Co reaction deduced from the experimental data under two different assumptions. Open circles are obtained from the average removed mass $\overline{\Delta A}$ and the assumption that the fractional transferred mass and linear momentum are equal. Solid circles are obtained using the assumption that the fractional transferred energy and linear momentum are equal. The indicated error bars do *not* include the measurement uncertainties in average mass removal and momentum transfer, but rather reflect only the uncertainty in the number of nucleons in the thermalized system, corresponding to the assumption that the recoiling mass is equal to the mass of the compound nucleus (lower limit) or to the mass of the target (upper limit).

IV. DISCUSSION

The gross structure of the data presented in this paper clearly indicates at least three different reaction regimes for the interaction of ^{4}He projectiles with a ^{59}Co target. The boundaries of these regimes are identified by abrupt changes in at least one experimental observable. The first regime extends from threshold up to about 10 MeV/nucleon bombarding energy, with $\overline{\Delta A}$ values, recoil ranges of individual reaction products, and the average momentum transfer (extrapolated to low energies) all suggesting the dominance of compound nucleus formation and subsequent decay by particle evaporation. Viola *et al.*[39] reached similar conclusions based on fission-fragment angular correlation measurements in the reaction of ^{4}He, ^{12}C, ^{16}O, and ^{20}Ne with uranium in the energy range from 7 to 35 MeV/nucleon. However, as has been pointed out by Duek *et al.*,[40] results of the analysis of 8.6 MeV/nucleon ^{20}Ne incident on ^{197}Au angular correlations indicate that a substantial fraction of fission reactions follows the incomplete fusion.

The second reaction regime extends from about 10 MeV/nucleon up to 23 MeV/nucleon bombarding energy. At 10 MeV/nucleon the variation of $\overline{\Delta A}$ and $\overline{\Delta Z}$ with α-particle energy changes slope, and the recoil ranges of individual reaction products begin to deviate significantly from the values expected for compound nucleus formation. However, in this energy range the formation of the compound nucleus still accounts for an appreciable frac-

tion of σ_{reac}, as indicated by the large values of the maximum momentum transfer. The contributions of complete fusion are much smaller in heavy ion induced reactions on heavy targets.[41,42] In order to see if there is really a target mass dependence of LMT, the data from reactions on medium mass nuclei ($A=100-150$) are necessary.

At approximately 23 MeV/nucleon a third regime sets in. Above this energy the average LMT begins to decrease with increasing bombarding energy and the maximum momentum transfer saturates (see Fig. 13), indicating that complete fusion is no longer significant above this energy. Also, at this bombarding energy, a change in the energy deposition mechanism seems to occur (see Fig. 16), although, as discussed in the preceding section, we are unable to say whether this change reflects an absolute decrease in the energy deposition rate or rather appears in the relationship between energy and linear momentum deposition.

In the ^{3}He+Co reaction a pattern similar to that for ^{4}He+Co is observed in the average and maximum LMT but, as indicated in Fig. 14, the change in the reaction regime takes place at somewhat higher bombarding energy per nucleon ($\approx$33 MeV/nucleon). However, for both projectiles this change is observed at roughly the same bombarding energy (95±5 MeV). It is also worth noting that the saturation values of the transferred linear momentum are similar (800±60 MeV/c) for both projectiles. The small difference in these values (760 MeV/c for ^{3}He and 860 MeV/c for ^{4}He projectile) may be significant when compared with heavier ion data, from which the saturation value of the LMT has been determined to be close to 2 GeV/c.[30]

Based on the data presented here as well as on the accumulated evidence from other work, the change of the reaction mechanism observed at about 40 MeV ^{4}He bombarding energy may be accounted for mainly by the onset of preequilibrium α-particle and nucleon emission. It is more difficult to infer the nature of the reaction mechanism change which occurs above 95 MeV bombarding energy and gives rise to the decrease of the average transferred linear momentum and the saturation of its maximum value. This transition might be associated with absorptive break-up[43,44] of the ^{4}He and ^{3}He projectile, a process known[45] to increase strongly with the bombarding energy. The measurements of the *differential* recoil ranges using the thin target–thin catcher technique, presently underway, will most probably elucidate whether the saturation of the maximum linear momentum transfer observed at this energy is indeed accompanied by the total disappearance of complete fusion. However, more systematic data on other target and projectile systems as well as model calculations will be necessary in order to understand microscopically the observed effect, which may be related to the expected[17] transition between mean field phenomena and individual nucleon-nucleon collisions.

V. SUMMARY AND CONCLUSIONS

The measurements reported in this paper extend substantially the previously existing information about ^{4}He and ^{3}He interactions with medium-mass nuclei. Cross section data obtained from in-beam γ-ray measurements and from radioactive decays were used to deduce the mass and charge distribution of residues, the average removed mass, and the average removed charge for ^{4}He reactions on a ^{59}Co target. These observables are related to the energy deposition during the interaction of the α particle with the target nucleus.

From the measured recoil ranges of the radioactive products information about the linear momentum transfer from the He projectiles to the target was gathered. The energy dependence of the average and maximum linear momentum transfer was investigated in detail.

Combining, under certain assumptions, the information about the linear momentum transfer and the average removed mass, we were able to deduce the average energy deposition in the thermalized composite system remaining after the fast reaction phase.

The comparison of the average removed mass and charge for proton, ^{4}He, ^{6}Li, and ^{13}C projectiles indicates that the energy deposition, for a given value of the bombarding energy, increases progressively with the mass of the projectile. For the ^{4}He projectile both the average removed mass and charge show a clear change in their energy dependence at about 40 MeV. This change in the reaction mechanism is attributed to the onset of preequilibrium particle emission.

Another change in the reaction mechanism appears to be effective above about 90 MeV incident energy for ^{3}He and ^{4}He projectiles. Experimentally, it is revealed by a distinct change in the behavior of the linear momentum transfers. The nature of this mechanism change is not clear at present. Its relation to the expected transition between mean field phenomena and individual nucleon-nucleon collisions needs further investigation.

ACKNOWLEDGMENTS

The authors appreciate the collaboration with Kernfysisch Versneller Institut (KVI), Groningen, in the preliminary stages of this work, where the first measurements of the recoil ranges in the ^{4}He+^{59}Co reaction were performed. They are also indebted to Dr. T. Ward for help in various stages of this work, and to Mr. B. Lozowski for the preparation of numerous targets employed here. This work was supported by the National Science Foundation under Grant No. PHY-81-14339, by Maria Curie Sklodowska Foundation Research Contract No. J-F7F059-P, and by the U.S. Department of Energy under Contract No. DE-AS05-76ER02408.

*On leave from the Institute for Nuclear Research, Swierk near Warsaw, Poland.

[1]M. Sadler, J. Jastrzębski, A. Nadasen, P. P. Singh, L. L. Rutledge, T. Chen, and R. E. Segel, Phys. Rev. Lett. **38**, 950 (1977).

[2]M. E. Sadler, P. P. Singh, J. Jastrzębski, L. L. Rutledge, and R. E. Segel, Phys. Rev. C **21**, 2303 (1980).

[3]J. Jastrzebski, H. Karwowski, M. Sadler, and P. P. Singh,

Phys. Rev. C **22**, 1443 (1980).
[4]J. Jastrzębski, H. Karwowski, M. Sadler, and P. P. Singh, Phys. Rev. C **19**, 724 (1979).
[5]M. Fatyga, J. Jastrzębski, H. Karwowski, T. Mróz, P. P. Singh, and S. E. Vigdor, in Proceedings of the International Conference on Nuclear Physics, Florence, 1983, Vol. 1, p. 535.
[6]J. Jastrzębski, P. P. Singh, T. Mróz, H. Karwowski, S. E. Vigdor, and M. Fatyga, Phys. Lett. **136B**, 153 (1984).
[7]R. Michel and G. Brinkmann, Nucl. Phys. **A338**, 167 (1980).
[8]E. Gadioli, E. Gadioli Erba, J. Asher, and D. J. Parker, Z. Phys. A **317**, 155 (1984).
[9]R. Michel and M. Glas, Nucl. Phys. **A404**, 77 (1983).
[10]F. Saint Laurent, M. Conjeaud, R. Dayras, S. Harar, H. Oeschler, and C. Volant, Phys. Lett. **110B**, 372 (1982).
[11]V. E. Viola, Jr., Lectures presented at the XVth Masurian Summer School on Nuclear Physics, Mikolajki, Poland, 1983.
[12]M. Blann, Phys. Rev. C **31**, 1245 (1985).
[13]E. Gadioli, E. Gadioli Erba, D. J. Parker, and J. Asher, Phys. Rev. C **32**, 1214 (1985).
[14]J. M. Alexander, in *Nuclear Chemistry,* edited by L. Yaffe (Academic, New York, 1968), Vol. I, p. 273.
[15]J. M. Alexander and G. N. Simonoff, Phys. Rev. **133B**, 93 (1964).
[16]M. Fatyga, diploma work, Institute for Nuclear Research, Swierk, 1980 (unpublished).
[17]D. K. Scott, Nucl. Phys. **A354**, 375 (1981).
[18]J. F. Ziegler, *The Stopping and Ranges of Ions in Matter* (Pergamon, New York, 1977), Vol. 4, p. 69.
[19]H. J. Probst, S. M. Qaim, and R. Weinreich, Int. J. App. Radiat. Isotopes **27**, 431 (1976).
[20]L. C. Northcliffe and R. F. Schilling, Nucl. Data Tables **7**, 233 (1970).
[21]L. Winsberg and J. M. Alexander, Phys. Rev. **121**, 518 (1961).
[22]C. M. Perey and F. G. Perey, At. Data Nucl. Data Tables **17**, 1 (1976).
[23]A. D'Onofrio, H. Dumont, M.-G. Saint Laurent, B. Delauny, F. Terrasi, and J. Delauny, Nucl. Phys. **A378**, 111 (1982).
[24]R. Kossakowski, J. Jastrzębski, P. Rymuza, W. Skulski, A. Gizon, S. André, J. Genevey, J. Gizon, and V. Barci, Phys. Rev. C **32**, 1612 (1985).
[25]W. Skulski *et al.* (unpublished).
[26]P. D. Croft, J. M. Alexander, and K. Street, Phys. Rev. **165**, 1380 (1968).
[27]J. M. Alexander and J. B. Natowitz, Phys. Rev. **188**, 1842 (1969).
[28]Y. Chan, M. Murphy, R. G. Stockstad, I. Tserruya, S. Wald, and A. Budzanowski, Phys. Rev. C **27**, 447 (1983).
[29]H. Morgenstern, W. Bohne, K. Grabisch, D. G. Kovar, and H. Lehr, Phys. Lett. **113B**, 463 (1982).
[30]J. Galin, H. Oeschler, S. Song, B. Borderie, M. F. Rivet, I. Forest, R. Bimbot, D. Gardes, B. Gatty, H. Guillemot, M. Lefort, B. Tamain, and X. Tarrago, Phys. Rev. Lett. **48**, 1787 (1982).
[31]D. J. Parker, J. Asher, T. W. Conlon, and I. Nagib, Phys. Lett. **116B**, 397 (1982).
[32]J. P. Bondorf, J. N. De, G. Fai, A. O. T. Karvinen, B. Jakobsson, and J. Randrup, Nucl. Phys. **A333**, 285 (1980).
[33]J. M. Alexander, C. Baltzinger, and M. F. Gazdik, Phys. Rev. **129**, 1826 (1961).
[34]M. Lagarde-Simonoff, S. Regnier, H. Sauvageon, and G. N. Simonoff, Nucl. Phys. **A260**, 369 (1976).
[35]T. Lund, D. Molzahn, B. Bergersen, T. Biørnstad, E. Hagebø, I. R. Haldorsen, and C. Richard-Serre, Phys. Lett. **116B**, 325 (1982).
[36]N. T. Porile, Phys. Rev. **120**, 572 (1960).
[37]K. Chen, Z. Frankel, G. Friedlander, J. R. Grover, J. M. Miller, and Y. Shimamoto, Phys. Rev. **166**, 949 (1968).
[38]G. Auger, D. Jouan, E. Plagnol, F. Pougheon, F. Naulin, H. Doubre, and C. Grégoire, Z. Phys. A **321**, 243 (1985).
[39]V. E. Viola, B. B. Back, K. L. Wolf, T. C. Awes, C. K. Gelbke, and H. Breuer, Phys. Rev. C **26**, 178 (1982).
[40]E. Duek, L. Kowalski, M. Rajagopalan, J. M. Alexander, D. Logan, M. S. Zisman, and M. Kaplan, Z. Phys. A **307**, 221 (1982).
[41]J. M. Alexander, E. Duek, and L. Kowalski, Z. Phys. A **323**, 83 (1986).
[42]M. B. Tsang, D. R. Klesh, C. B. Chitwood, D. J. Fields, W. G. Lynch, H. Utsunomiya, K. Kwiatkowski, V. E. Viola, and M. Fatyga, Phys. Lett. **134B**, 169 (1984).
[43]J. R. Wu, C. C. Chang, and H. D. Holmgren, Phys. Rev. Lett. **40**, 1013 (1978).
[44]A. Budzanowski, G. Baur, C. Alderliesten, J. Bojowald, C. Mayer-Boricke, W. Oelert, P. Turek, F. Rosel, and D. Trautmann, Phys. Rev. Lett. **41**, 635 (1978).
[45]J. R. Wu, C. C. Chang, H. D. Holmgren, and R. W. Koontz, Phys. Rev. C **20**, 1284 (1979).